NASA TECHNICAL NOTE

NASA TN D-6327

COMBINED ELECTRON MICROSCOPE, ELECTRON DIFFRACTION, AND ELECTRON MICROPROBE ANALYSIS OF IDENTICAL MICROSTRUCTURES IN THE DEBOND AREA OF A DISSIMILAR METAL JOINT

by L. G. Bostwick and R. Burton

John F. Kennedy Space Center
Kennedy Space Center, Fla. 32899

NATIONAL AERONAUTICS AND SPACE ADMINISTRATION • WASHINGTON, D. C. • AUGUST 1971

1. Report No.	2. Government Accession No.	3. Recipient's Catalog No.
NASA TN D-6327		

4. Title and Subtitle	5. Report Date
Combined Electron Microscope, Electron Diffraction, and Electron Microprobe Analysis of Identical Microstructures in the Debond Area of a Dissimilar Metal Joint	August 1971
	6. Performing Organization Code

7. Author(s)	8. Performing Organization Report No.
L. G. Bostwick and R. Burton	

9. Performing Organization Name and Address	10. Work Unit No.
John F. Kennedy Space Center, Fla.	11. Contract or Grant No.
	13. Type of Report and Period Covered
12. Sponsoring Agency Name and Address	Technical Note
National Aeronautics and Space Administration	14. Sponsoring Agency Code

15. Supplementary Notes

Prepared by Support Operations Laboratory, Materials Analysis Branch

16. Abstract

The examination of a defective solid state weldment on a liquid hydrogen tank from the Apollo 12 fuel cell system was undertaken to supplement results of an earlier malfunction investigation.

Correlation of data accumulated on identical microstructures by electron microscopy, electron diffraction, and electron microprobe analysis resulted in the identification of numerous anomalous constituents in the weld interface zone, thereby demonstrating the feasibility of applying this unique combination of techniques to the identification of unknown particulates.

17. KeyWords	18. Distribution Statement
Electron Microscope Electron Microprobe Photomacrograph Electron Micrograph Particle Cluster X-ray Scan	Unlimited Distribution

19. Security Classif. (of this report)	20. Security Classif. (of this page)	21. No. of Pages	22. Price *
Unclassified	Unclassified	22	3.00

CONTENTS

COMBINED ELECTRON MICROSCOPE, ELECTRON DIFFRACTION, AND ELECTRON MICROPROBE ANALYSIS OF IDENTICAL MICRO-STRUCTURES IN THE DEBOND AREA OF A DISSIMILAR METAL JOINT

by
L. G. Bostwick and R. Burton
John F. Kennedy Space Center, Fla.

INTRODUCTION

The successful application of a combination of electron microscope and electron microprobe techniques to the solution of diverse analytical problems has been reported in the technical literature by numerous investigators (References 1-6).

In the cited investigations, the identity of preselected areas or structures is generally established by correlating microstructural characteristics, defined by the electron microscope, with the elemental composition determined by the electron microprobe.

A similar approach, supplemented by the application of transmission electron diffraction, was employed in this study. Inclusion of the electron diffraction data made it possible to determine the chemical composition of preselected microstructures with an accuracy not attainable with conventional electron microscope/electron microprobe technique.

The opportunity to employ the combination of the three techniques presented itself during the course of a study undertaken to supplement the results obtained in an earlier malfunction investigation of a defective liquid hydrogen storage tank (Figure 1) of the Apollo 12 Command Service Module Fuel Cell Hydrogen System.

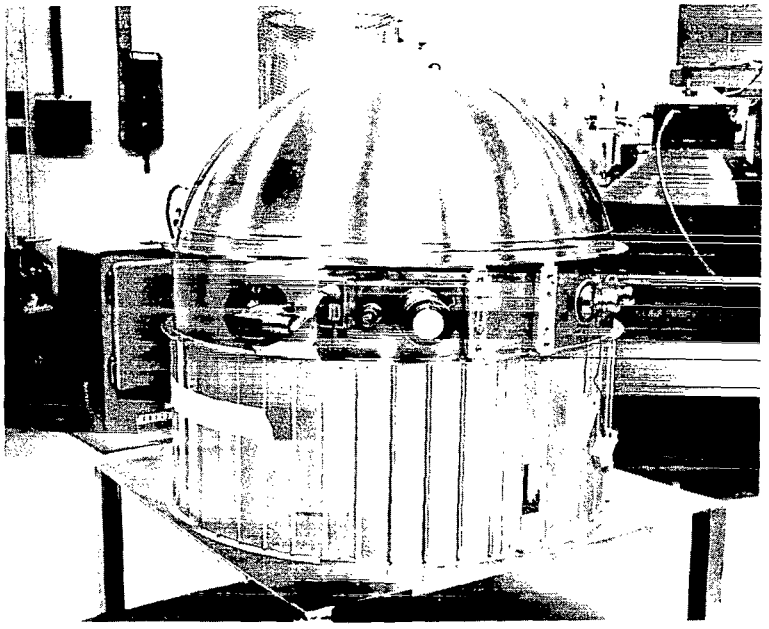

Figure 1. Liquid Hydrogen Storage Tank, P/N ME-282-0047-0050, S/N 0001, Apollo 12 Command Service Module Fuel Cell Hydrogen System
Scale: 1" = 1' 3"

In the original investigation (Reference 7), tank malfunction was traced to a leak path in the manifold area at the interface of the solid state weld between the titanium alloy tank and the stainless steel inlet/outlet port (Figure 2).

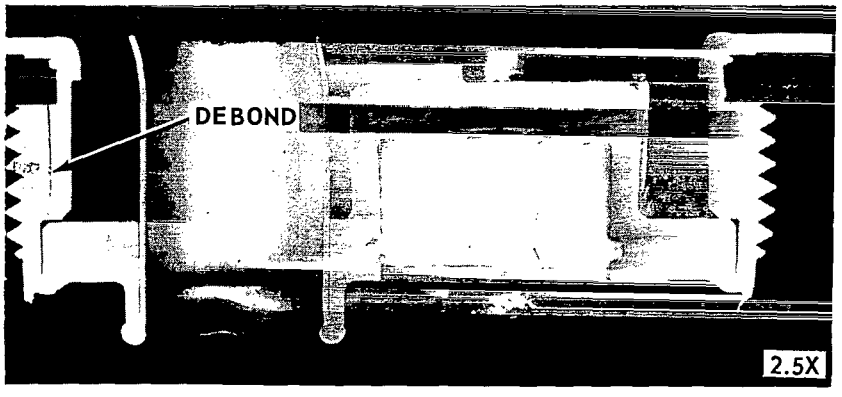

Figure 2. Photomacrograph of the manifold cross-section depicting area of debond which formed the leak path

Electron microprobe examination of a polished section through the defective bond region (Figure 3), performed in the original investigation, revealed the presence of small, highly localized oxygen-rich structures at the weld interface. Further characterization of these structures was not attempted in the original survey.

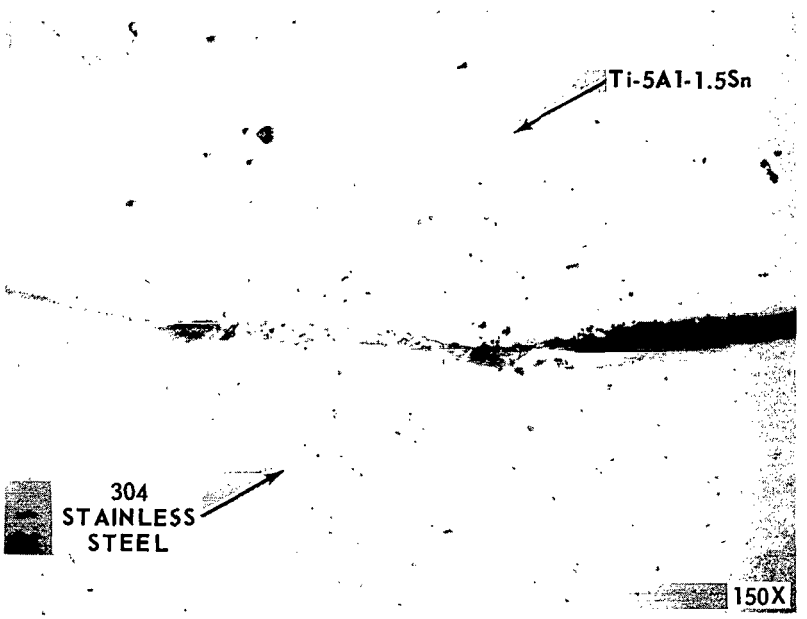

Figure 3. Polished section through defective bond region showing small, highly localized oxygen-rich structures at the weld interface

The intent of this study was to perform a detailed reinvestigation of the failed weld interface to characterize the interface contaminant more precisely, by (1) determining the exact nature of the oxygen-rich structures observed in the original study, and by (2) conducting a survey for, and identifying, any additional anomalous constituents present in the weld interface microstructure.

EXPERIMENTAL DETAILS

The polished section through the defective bond region (Figure 4), prepared for metallurgical evaluation in the original malfunction investigation (Reference 7), was also used in this study.

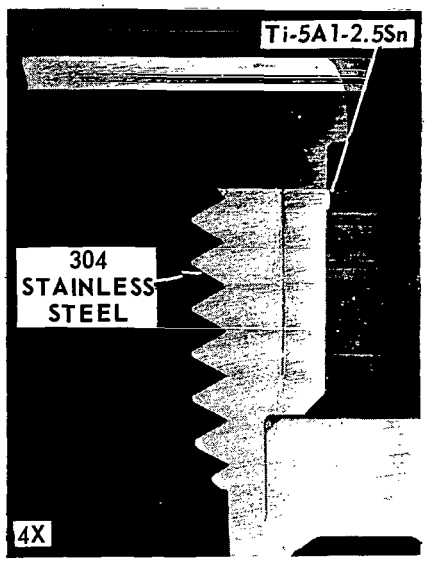

Figure 4. Photomacrograph of liquid hydrogen tank manifold, showing debond area at the titanium alloy tank/stainless steel inlet/outlet port interface

The stainless steel and titanium alloy components were mechanically separated and replicas of the freshly fractured surfaces were immediately prepared by the conventional two-stage acetate replica technique.

A strip of Faxfilm® (cellulose acetate) moistened with acetone was pressed onto each fracture surface and allowed to dry. The acetate films were then stripped from the surfaces, placed in a vacuum evaporator and coated with a thin carbon film. These compound replicas were then cut into 1/8-inch squares and the acetate layer dissolved by immersing the squares in an acetone-water (80:20) bath. The individual replicas were then readied for instrumental analysis by mounting on standard 200 mesh copper grids.

Examination of the replicas was divided into three phases.

1. Representative particles extracted from each fracture surface were located and photographed at magnifications of 8,100X and 18,500X in the electron microscope.

2. The replicas were then examined in the electron microprobe where representative particles were randomly selected and surveyed for elemental composition.

3. The replicas were then returned to the electron microscope and electron diffraction data obtained on the identical particles previously surveyed in the electron microprobe.

DISCUSSION

Phase 1: Electron Microscopy, Preliminary Survey

Typical electron micrographs of randomly selected representative particles extracted from the fractured weld surfaces are presented in Figures 5 and 6.

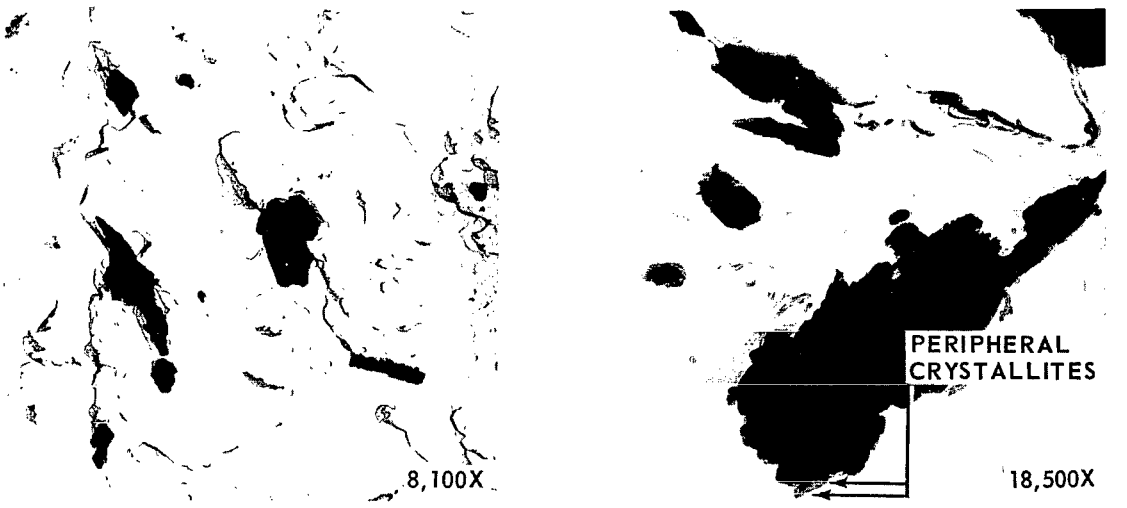

Figure 5. Electron Micrographs: Typical particles extracted from fractured surface of the stainless steel weld member

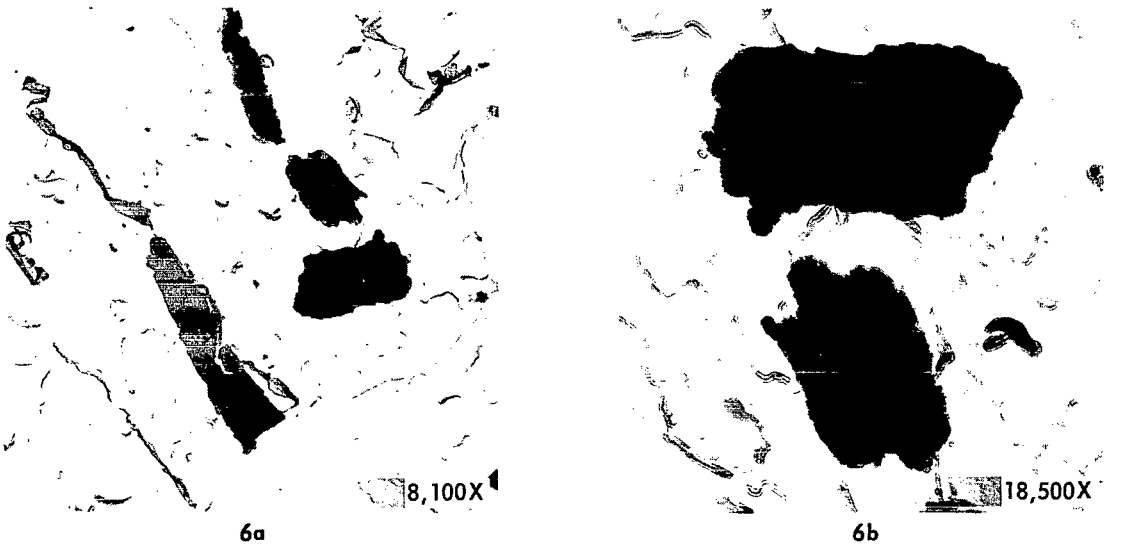

Figure 6. Electron Micrographs: Typical particles extracted from fractured surface of the titanium alloy weld member

An inspection of Figures 5 and 6 reveals the following:

1. The morphology of the particles extracted from the fractured surfaces of both weld members is very similar.

2. The large particles are seen to consist of an aggregate of small crystallites (Figure 5b).

In reference to the sharply defined electron diffraction patterns obtained in a later phase of this study, it is noted here that the patterns were produced by individual crystallites of the type located at the peripheries of the large particles.

Phase 2. Electron Microprobe Analysis

Following the initial electron microscope survey, the two replicas were transferred to the electron microprobe for elemental characterization. This was accomplished in three steps:

1. Location and selection of representative particles on each replica, employing backscattered electron imaging techniques.

2. Analysis of selected particles to obtain qualitative information regarding their elemental composition.

3. Use of X-ray imaging techniques to determine the relative concentration and distribution of the elemental constituents known to be present in the particles.

Summary of Electron Microprobe Data

1. Stainless Steel Fracture Surface Replica

A cluster of three particles was randomly selected for analysis. An analysis of the individual particles in the cluster revealed that the particles consisted primarily of titanium and iron. They also contained heterogeneously distributed secondary concentrations of oxygen and minor-to-trace quantities of chromium, nickel, and manganese.

The relative concentration and distribution of these elements in each particle were then determined by conventional X-ray imaging techniques. Selected element distributions (Ti, Fe, Cr, Ni) obtained in this manner are presented in Figure 7.

Element distribution images are not included for oxygen and manganese. Poor signal-to-noise ratios for these elements precluded clear-cut photographic imaging of their distributions in the particles.

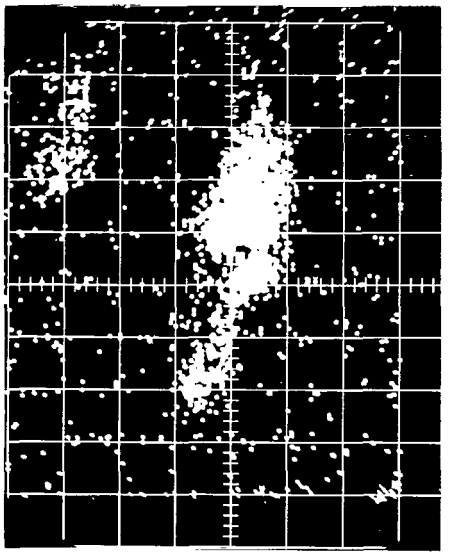

Fe Kα
X-RAY SCAN

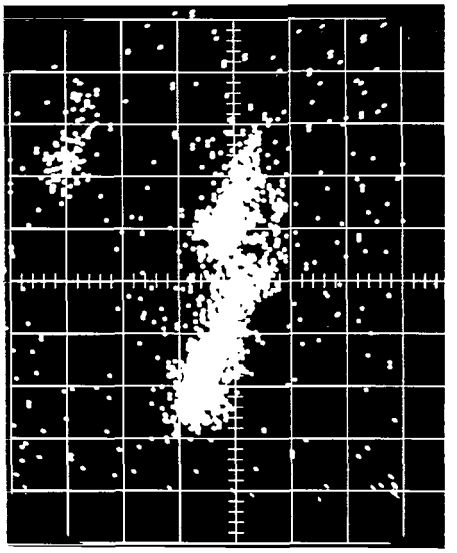

Ti Kα
X-RAY SCAN

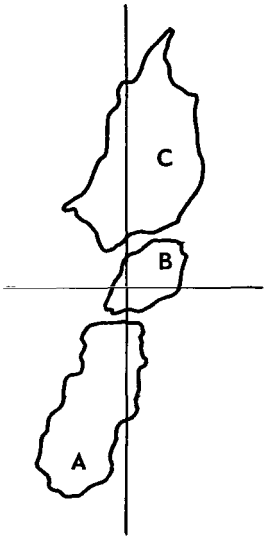

KEY TO
PARTICLE IDENTITY

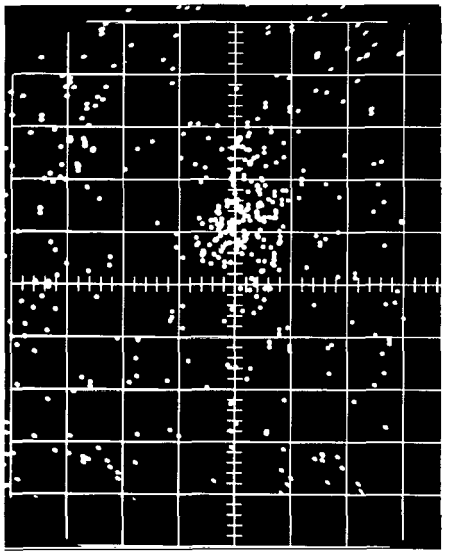

Cr Kα
X-RAY SCAN

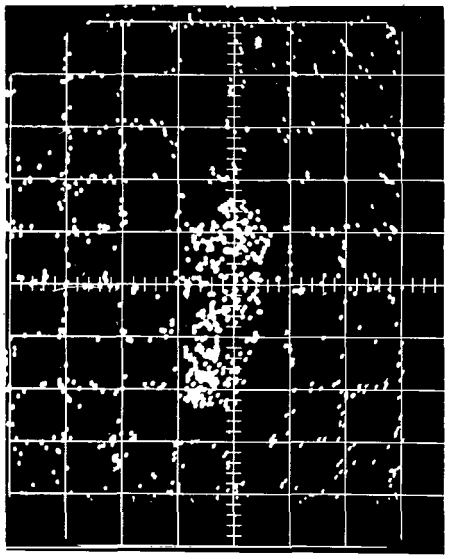

Ni Kα
X-RAY SCAN

Figure 7. X-ray scan images showing Fe, Ti, Cr, and Ni distributions in individual members of particle cluster, stainless steel fracture surface replica. Image magnification: 4000X. Key to particle identity: Letter designations arbitrarily assigned to facilitate correlation of electron microprobe and electron diffraction data.

Based upon an evaluation of the X-ray scan images presented in Figure 7, the following generalizations can be made with respect to Fe, Ti, Cr, and Ni concentration and distribution in the individual particles.

Particle A: Major Ti, with associated minor Fe. General localization of Fe evident in central portion of particle. Ni is present in diffuse trace range. Cr absent. (From Static Probe Data: Heterogeneous minor O_2 and traces of Mn also present.)

Particle B: Major Fe, Ti. Minor-to-trace level Ni and Cr present. (From Static Probe Data: Heterogeneous minor O_2 and traces of Mn also present.)

Particle C: Major Fe, with associated minor Ti. General localization of Ti evident in left lateral portion of particle. Minor-to-trace level Ni and Cr present. (From Static Probe Data: Heterogeneous minor O_2 and traces of Mn also present.)

Major: > 10%

Minor: 1 - 10%

Trace: < 1%

2. Titanium Fracture Surface Replica

A two-particle cluster was selected for analysis. Static probe and X-ray imaging techniques were employed to determine the chemical content of the particles. The data obtained by these techniques showed the two particles to bear a striking similarity to the particles analyzed on the stainless steel fracture surface replica. Like their stainless steel counterparts, these particles were found to contain heterogeneously distributed major Fe and Ti, minor O_2, minor-to-trace Cr and Ni, and traces of Mn. Corroborating X-ray images, showing the relative concentration and distribution of Fe, Ti, Cr, and Ni in the particles, are presented in Figure 8.

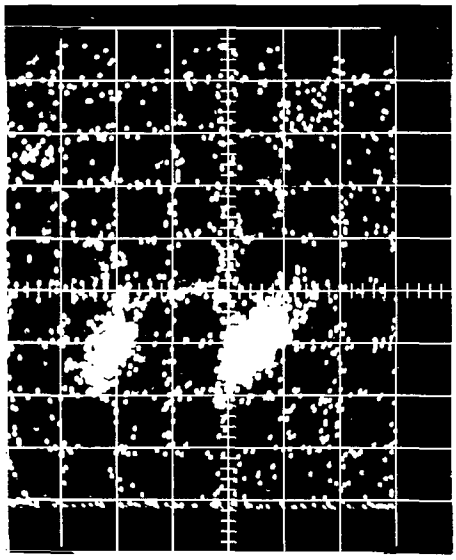

Fe Kα
X-RAY SCAN

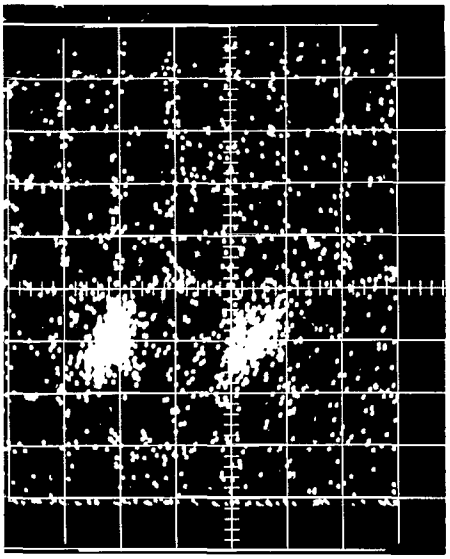

Ti Kα
X-RAY SCAN

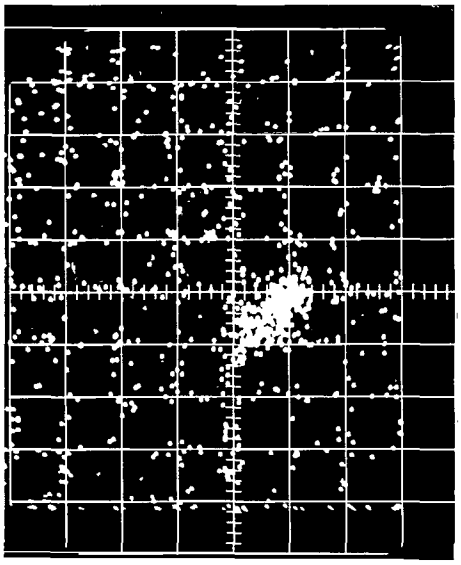

Cr Kα
X-RAY SCAN

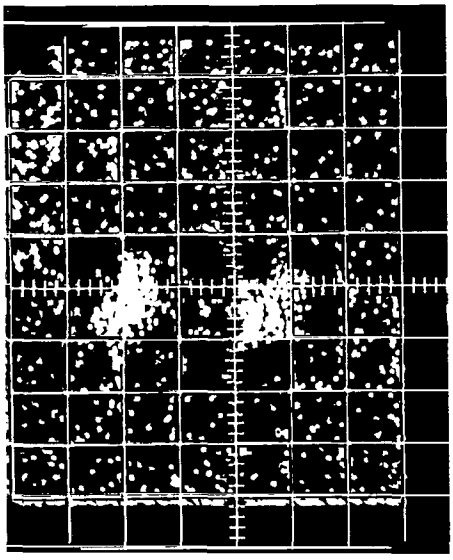

Ni Kα
X-RAY SCAN

Figure 8. X-ray scan images showing Fe, Ti, Cr, and Ni distributions in individual members of particle cluster, titanium fracture surface replica. Image magnification: 4000X

Phase 3. Electron Diffraction Analysis

Upon completion of the electron microprobe analysis, the two replicas were returned to the electron microscope for electron diffraction analysis. This was to be accomplished in two steps: (1) location and photography of the specific particles analyzed in the electron microprobe and (2) electron diffraction analysis of the particles.

Summary of Phase 3 Analysis

1. Stainless Steel Fracture Surface Replica

The specific replica surface region containing the three-particle cluster of interest was rapidly identified by locating the contamination film* deposited on the replica surface during the electron microprobe analysis.

A typical contamination film is shown in Figure 9.

Figure 9. Typical contamination film (outlined area) formed by carbon deposition on the replica surface during electron microprobe analysis (cf. footnote, page 11).

*Formed by the deposition of the decomposition product (primarily carbon) produced by the interaction of the electron beam with vacuum pump oil molecules on or near the specimen surface.

Once the contamination film was located, the three-particle cluster was readily identified and photographed. Figure 10 is an electron micrograph of the three-particle cluster.

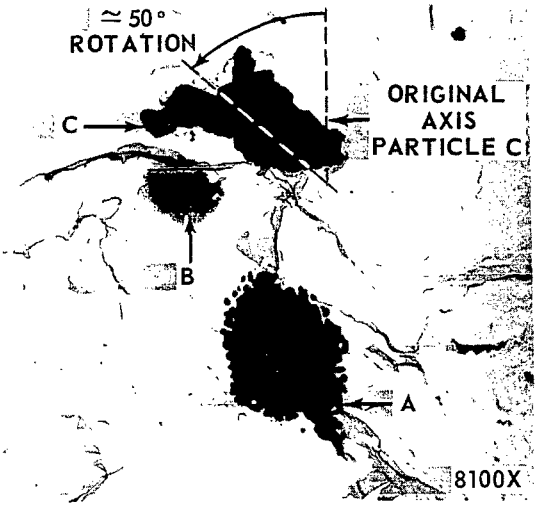

Figure 10. Electron micrograph, three-particle cluster analyzed in the electron microprobe

Note: (1) To permit unambiguous correlation of electron microprobe and electron diffraction data, particle identification corresponds to that used in Figure 7.

(2) Figure 10 is a mirror image of the three-particle cluster as shown in each of the X-ray scan images presented in Figure 7. Additionally, rupture (irregular white region) of the substrate film subsequent to the electron microprobe analysis has resulted in an approximate 50-degree counterclockwise rotation of particle C from its original position in the substrate.

Peripheral crystallites of particles A, B, and C all produced sharply defined electron diffraction patterns of the type shown in Figure 11.

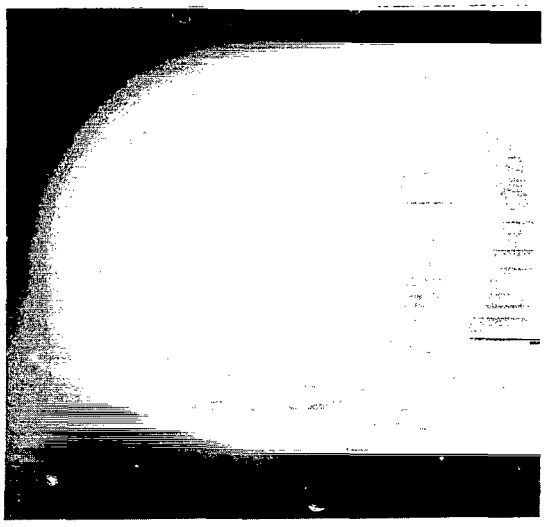

Figure 11. Electron diffraction pattern, particle B, stainless steel weld member fracture surface replica

The identification of specific compounds from the "d" values calculated from the electron diffraction patterns was based upon information in the "Inorganic Index to the Powder Diffraction File" (Reference 8). Diffraction data are presented in Table 1 (Appendix).

In summary, peripheral crystallites of particle A produced a pattern identified as rutile (titanium dioxide, TiO_2).

Pooled data from randomly selected peripheral crystallites of particle B indicate it to be a complex aggregate of at least three constituents: alpha iron (αFe), titanium (Ti), and the compound iron titanate ($FeTiO_5$).

Data from peripheral crystallites of particle C indicate the presence of titanium (Ti) and alpha iron oxide hydrate [$\alpha FeO(OH)$].

2. Titanium Fracture Surface Replica

The two-particle cluster examined in the electron microprobe is shown in Figure 12.

Figure 12. Electron micrograph, two-particle cluster analyzed in the electron microprobe

As a result of the catastrophic rupturing of the supporting substrate and the concomitant severe degree of particle fragmentation and reorientation evidenced in Figure 12, phase 3 studies were restricted to photography of the cluster. No attempt was made to collect electron diffraction data on these specific particles. However, in order to provide electron diffraction data for comparison against that accumulated for the stainless steel replica particles, electron diffraction analysis was performed on several randomly selected particles located in an unruptured region of the titanium weld surface replica.

An analysis of the electron diffraction patterns produced by these particles showed them to contain the following chemical entities: alpha iron (αFe), iron oxide (FeO), iron titanium oxide (Fe_2Ti_4O), and titanium dioxide (TiO_2).

3. Comparison of Analytical Data

A comparison of the compounds identified in the particles examined on both replicas shows the following marked similarities.

a. Particles on the two substrates exist both in simple metal or single compound form and as complex aggregates of metal(s) and metal oxidation products.

b. Predominant oxidation products common to both substrate particles are iron oxides, titanium dioxide, and iron-titanium oxides.

CONCLUSIONS

Electron microprobe analysis combined with electron microscopy and electron diffraction analysis comprise a unique method for the precise identification of unknown particulates present on standard replicas such as those normally prepared for electron microscopy. The feasibility of this integrated approach has been demonstrated by its application to the analysis of diverse foreign particles extracted from the interface region of a defective solid state weldment.

In terms of future applications of this technique, it is recommended that precautions be taken to insure against catastrophic rupture of the delicate substrate film induced by localized thermal effects. For example, use of the thickest carbon substrate film compatible with the execution of interference-free electron diffraction procedures is recommended to alleviate this problem.

REFERENCES

1. A. W. Hull, "X-Ray Microanalysis of a Radioactive Particle with the Aid of the Electron Microscope," Nature, 195, pp. 369-70, 1962.

2. L. S. Birks, "Electron Probe Microanalysis," pp. 154-155, Interscience Publishers, New York, 1963.

3. J. R. Shapiro, "Electron Probe Microanalysis of Zinc-bearing Hexagonal Ferrites" in "Advances in X-Ray Analysis" Vol. 9, pp. 304-313, Plenum Press, New York, 1965.

4. U. Gerloff, J. H. Weibraugh and H. Fechtig, "Electron Microscope and Microprobe Measurements on Luster-Flight Samples" in "Space Research VII," Vol. II, Part XI, pp. 1412-20, North Holland Publishing Company, Amsterdam, 1967.

5. M. M. Robertson and W. B. Estill, "Electron Probe and Electron Microscope Investigation of Identical Areas" in "First National Conference on Electron Probe Microanalysis," Paper No. 39, College Park, Maryland, May 4-6, 1966.

6. K. H. Meyer, K. Stulpe, and J. P. Lehner, "Investigation of Interfaces Between Steel and Vapor Phase Deposited Tungsten by Optical and Electron Microscopy and by Electron Probe Microanalysis," in "Proceedings - Electron Microscopy Society of America - Twenty-sixth Annual Meeting," pp. 394-95, September 1968.

7. J. T. Copeland and C. R. Denaburg, Malfunction Investigation Report MAB-365-69, John F. Kennedy Space Center, Florida, November 18, 1969.

8. "Inorganic Index to the Powder Diffraction File," Publication PD1S-20i, Joint Committee on Powder Diffraction Standards, 1970.

APPENDIX

Table 1
Electron Diffraction Data
Stainless Steel Section

Particle A[1]	TiO_2 Rutile[3] 4-0551	Particle B[2]	Fe_2TiO_5 9-182[3]	Ti 5-0682[3]	αFe 6-0696[3]	Particle C	αFeO(OH) 17-536[3]
		4.96	4.90[45]	-	-	5.30	5.00[10]
		3.74	-	-	-	4.19	4.18[100]
		3.41	3.48[100]	-	-	-	3.38[10]
-	3.24[100]	3.06	-	-	-	3.19	-
2.46	2.49[41]	2.75	2.75[80]	-	-	3.06	-
2.39	-	2.57	-	2.56[30]	-	3.02	-
2.18	2.18[22]	-	2.40[25]	2.34[26]	-	2.99	-
2.06	2.05[9]	2.23	2.22[11]	2.24[100]	-	2.80	-
1.68	1.69[50]	-	2.19[15]	-	-	2.79	-
1.65	-	2.08	-	-	2.03[100]	2.68	2.69[30]
1.60	1.62[16]	1.88	1.86[30]	-	-	2.61	2.58[8]
1.57	-	1.78	1.74[15]	1.73[19]	-	-	2.49[16]
1.34	1.35[7]	1.50	1.49[11]	1.48[17]	-	-	2.52[4]
-	1.24[3]	1.46	1.42[15]	-	1.43[19]	-	2.45[25]
-	1.15[4]	-	-	1.33[16]	-	-	2.25[10]
-	1.12[4]	-	-	1.28[2]	-	2.18	2.19[20]
1.10	1.09[4]	1.24	1.24[5]	1.25[16]	-	2.16	-
1.09	1.08[4]	-	-	1.23[13]	-	2.06	2.01[2]
		1.16	-	1.17[2]	1.17[30]	-	1.92[6]
		1.12	-	1.12[2]	-	-	1.80[8]

Table 1 (Cont'd)
Electron Diffraction Data
Stainless Steel Section

Particle C	Ti 5-0682[3]	αFeO(OH) 17-536[3]
5.09	-	4.98[10]
4.20	-	4.18[100]
-	-	3.38[10]
3.13	-	-
3.06	-	-
2.79	-	-
2.67	-	2.69[30]
2.61	-	-
2.58	-	2.58[8]
2.56	2.56[30]	-
2.52	-	2.52[4]
-	2.34[26]	2.49[16]
-	-	2.45[25]
2.28	-	-
2.24	2.24[100]	2.25[10]
-	-	2.19[20]
1.72	1.73[19]	1.72[20]
-	-	1.69[10]
-	-	1.66[4]
-	-	1.61[6]
1.54	-	1.56[16]
1.52	-	1.51[10]
1.49	1.48[17]	1.47[4]
-	-	1.45[10]
-	-	1.42[2]
-	-	1.39[8]
1.36	-	1.36[8]
1.32	1.33[16]	1.32[8]
1.28	1.28[2]	1.26[2]
1.22	1.23[13]	1.24[2]
-	-	1.20[2]
1.16	1.17[2]	-
1.13	1.12[2]	-
1.06	1.07[3]	-
1.02	-	-
1.00	-	-
0.99	0.99[8]	-
0.97	-	-
0.96	-	-
0.95	0.95[12]	-
0.91	0.92[10]	-
0.90	0.89[4]	-
0.88	0.88[4]	-
-	0.86[3]	-
0.85	0.85[4]	-
0.82	0.82[12]	-

Table 1 (Cont'd)

Electron Diffraction Data

Stainless Steel Section

Particle A[1]	TiO_2 Rutile[3] 4-0551	Particle B[2]	Fe_2TiO_5 9-182[3]	Ti 5-0682[3]	αFe 6-0696[3]	Particle C	αFeO(OH) 17-536[3]
0.91	0.91[3]					1.77	1.77[2]
0.89	0.89[5]	1.07	-	1.07[3]	-	-	1.72[20]
-	0.88[6]	0.99	-	-	1.01[9]	1.69	1.69[10]
-	0.84[5]	0.97	-	0.97[6]	-	1.66	1.66[4]
-	0.82[8]	-	-	0.94[11]	-	-	1.61[6]
		0.89	-	0.89[4]	0.91[12]	1.57	1.56[16]
		0.87	-	0.88[4]	-	1.53	1.51[10]
		0.83	-	0.83[12]	0.83[6]	1.47	1.47[4]
						-	1.45[10]
						-	1.42[2]
						1.40	1.39[8]
						1.36	1.36[8]
						-	1.32[8]
						1.26	1.26[2]
						1.24	1.24[2]
						-	1.20[2]
						1.14	-
						1.12	-
						1.08	-
						0.96	-
						0.92	-
						0.90	-

[1]Electron Microprobe data - Fe+Ti, particle "A"

[2]Electron microprobe data - Ti+Fe+Ni+Cr, particle "B"

[3]ASTM X-Ray file card numbers

"The aeronautical and space activities of the United States shall be conducted so as to contribute . . . to the expansion of human knowledge of phenomena in the atmosphere and space. The Administration shall provide for the widest practicable and appropriate dissemination of information concerning its activities and the results thereof."

—NATIONAL AERONAUTICS AND SPACE ACT OF 1958

NASA SCIENTIFIC AND TECHNICAL PUBLICATIONS

TECHNICAL REPORTS: Scientific and technical information considered important, complete, and a lasting contribution to existing knowledge.

TECHNICAL NOTES: Information less broad in scope but nevertheless of importance as a contribution to existing knowledge.

TECHNICAL MEMORANDUMS: Information receiving limited distribution because of preliminary data, security classification, or other reasons.

CONTRACTOR REPORTS: Scientific and technical information generated under a NASA contract or grant and considered an important contribution to existing knowledge.

TECHNICAL TRANSLATIONS: Information published in a foreign language considered to merit NASA distribution in English.

SPECIAL PUBLICATIONS: Information derived from or of value to NASA activities. Publications include conference proceedings, monographs, data compilations, handbooks, sourcebooks, and special bibliographies.

TECHNOLOGY UTILIZATION PUBLICATIONS: Information on technology used by NASA that may be of particular interest in commercial and other non-aerospace applications. Publications include Tech Briefs, Technology Utilization Reports and Technology Surveys.

Details on the availability of these publications may be obtained from:

SCIENTIFIC AND TECHNICAL INFORMATION OFFICE

NATIONAL AERONAUTICS AND SPACE ADMINISTRATION

Washington, D.C. 20546